Journal of Materials Chemistry C

Accepted Manuscript

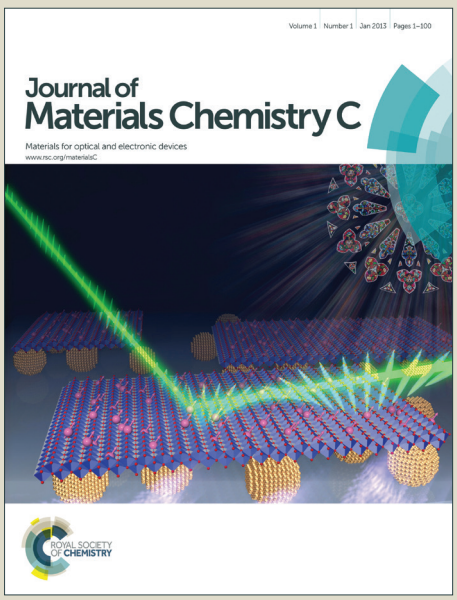

ROYAL SOCIETY OF CHEMISTRY

www.rsc.org/materialsC

J. Mater. Chem. C

Ultrafast Electron Transfer in Nanocomposite of Graphene Oxide-Au Nanocluster with Graphene Oxide As a Donor

Xiaoming Wen,[*1] *Pyng Yu,*[*2] *Yon-Rui Toh*[2], *Yu-Chieh Lee*[2], *Kuo-Yen Huang*[2], *Shujuan Huang*[1], *Santosh Shrestha*[1], *Gavin Conibeer*[1] *and Jau Tang*[*2]

[1]Australian Centre for Advanced Photovoltaics, University of New South Wales, Sydney 2052, Australia

[2]Research Center for Applied Sciences, Academia Sinica, Taipei, Taiwan

Keyword: Metallic nanoclusters, graphene oxide, electron transfer, ultrafast spectroscopy

Corresponding author:
x.wen@unsw.edu.au,
pyngyu@gate.sinica.edu.tw,
jautang@gate.sinica.edu.tw

Abstract

Graphene oxide has been extensively investigated as an electron acceptor due to its exceptional electronic and optical properties. Here we report an unusual ultrafast electron transfer occurring in the nanocomposites of Au nanocluster (Au NCs) - graphene oxide (GO) in which GO acts as an electron donor. An ultrafast electron transfer is corroborated from the excited states of graphene oxide into the highest occupied molecular orbital (HOMO) of Au NCs. It is found the electron transfer rate is significantly larger in Au_{10}-GO nanocomposites (4.17×10^{12} s^{-1}) than that in Au_{25}-GO (0.49×10^{12} s^{-1}) due to a larger energy difference and smaller sized ligands. This finding suggests that graphene oxide - Au nanocluster nanocomposites can be very useful to construct novel nanostructures with enhanced visible light photovoltaic, photonic and photo-catalytic activities.

Introduction

Graphene is a monolayer of tightly packed carbon atoms. Such a two-dimensional carbon nanomaterial has become the most promising materials due to its excellent electronic and ballistic electron transport features. Its exceptional fast mobility of electrons as well as broad spectral absorption offers promising applications in nano-electronics and photovoltaics.[1] In recent years, the water-soluble derivative of graphene, graphene oxide (GO), has attracted great attention to be potentially applied in photonics and photovoltaics because it exhibits partly similar electronic and optical properties; and importantly, the synthesis of GO is much easier and lower cost than that of graphene. Reduced GO (rGO) has been widely used for transparent conductor applications as possible replacement for indium tin oxide (ITO) in photovoltaic devices.[2] Few-layered GO has fast energy relaxation of hot carriers and strong saturable absorption, which is comparable with that of rGO.[3] It has been shown that GO exhibits strong hydrophobic interactions and unique surface irreversible protein adsorption ability; thus GO is a promising materials for accommodating proteins and facilitating protein electron transfer.[4-6] It is expected that GO sheets can provide unique 2-D architecture to be an excellent electron acceptor or donor. In particular, in GO carbon atoms bonded with oxygen groups are sp^3 hybridized, disrupting the sp^2 conjugation of the hexagonal graphene lattice. Consequently, the well-known linear dispersion of the Dirac electrons is destructed and the optical properties are modified.[7-8]

Gold nanoclusters (Au NCs) comprising several to tens of gold atoms have been shown to possess distinct optical, magnetic and catalytic properties and have attracted considerable research interest due to their fundamental importance and potential applications in catalysis, bioimaging and photovoltaics.[9-11] Due to the small size of Au NCs comparable to Fermi wavelength of electrons, the NCs exhibit discrete energy levels and molecule-like properties in the absorption and fluorescence features.[12-14] More importantly, Au NCs with a precisely controlled atom number have corresponding

structures and correlated optical properties.[15-17] Various Au NCs have been synthesized with a specific number of metal atoms according to the requested emission wavelength and ligand shells.[16-20] For example, it has been demonstrated that the small Au_{10} NCs consist of neutral Au atoms; while Au_{25} NCs have a core-semiring structure in which thirteen Au(0) atoms form a icosahedral core surrounded by six $Au_2(SR)_3$ staples.[16, 21-22] Such structures have been proven independent on the types of surface ligands.[12, 14] Effective electron transfer was observed in Au NCs based nanocomposites, which suggests Au NCs can be superior in photocatalysis and photovoltaics.[23-29] Sakai *et al*. observed that photoexcited electrons in $Au_{25}(SG)_{18}$ can be injected into the TiO_2 conduction band with a high internal quantum efficiency (~ 60%).[30] In a further study, the size dependent electronic structures of Au NCs and Au nanoparticles on TiO_2 were conducted by photocurrent measurements.[31] Recently, Kamat *et al*. demonstrated the Au NCs sensitized solar cells with an initial efficiency of 2%. [25]

Dynamic understanding for the photoinduced electron and energy transfer is of crucial importance because it can result in potential applications in photovoltaics, photo-catalysis, and other optical applications. [9, 14, 25, 32] Although electron transfer dynamics has been extensively studied in graphene and graphene oxide, as well as Au NCs based nanocomposites.[25] To date, only few studies have focused on graphene and GO as electron donors.[33-36] The basic understanding on the electron donor of GO is still lacking, particularly for electron transfer dynamics. Herein we study electron transfer dynamics in Au NCs-GO nanocomposites using steady state and ultrafast time-resolved spectroscopy. An effective fluorescence quenching was found in Au NCs-GO system and it is attributed to an unusual electron transfer to Au NCs from GO. This finding can be very useful for further construction of functionalized nanocomposites based on GO and Au NCs for the applications in photovoltaics, photonics and photocatalysis.

Results and Discussion

Fluorescence quenching has been widely used to probe photoinduced electron transfer in nanocomposites.[37-38] The Au NCs used in this study include bovine serum albumin (BSA) protected Au_{25} (Au_{25}/BSA) and histidine protected Au_{10} (Au_{10}/His). The synthesis details are described in experimental section. The size of Au10and the characterization details have been previously reported.[10, 17-18, 39-40] Transmission electron microscopy (TEM) images for Au_{25} NCs/GO and Au_{10} NCs/GO are showed in Figurer S1 in supporting information. It is clear that the both Au_{25} and Au_{10} NCs were attached onto GO, confirming the strong interaction between Au NCs and GO. Au_{25}/BSA has relatively larger size than Au_{10}/His, consistent with the previous studies. The PL spectra of Au_{25} and Au_{10} were observed around 650 and 530 nm, respectively. They also exhibit the featured lifetime. GO exhibits weak and broad PL in the visible region, similar to the other reports.[41-42]

Au_{25} NCs-GO nanocomposites

The PL spectra of Au_{25} NCs-GO mixture were measured as a function of the GO concentration. As shown in Figure 1a, the PL intensity of Au_{25} NCs monotonically decreases with increasing GO concentration; and the PL peak does not shift evidently. Significant PL quenching indicates the strong interaction between Au_{25} NCs and GO. In order to obtain the insight into the mechanism of PL quenching, the Stern-Volmer (S-V) plots, the peak intensity as a function of GO concentration, was shown in the inset of Figure 1a. The S-V plot exhibits approximately a linearity with a quenching constant of 0.75×10^3 $(\mu g/mL)^{-1}$.[43] In general, a linear Stern-Volmer behaviour can arise from either a dynamic or static mechanism.[44] The static quenching can result from formation of non-luminescent complex, while the dynamic quenching can arise from energy transfer, electron transfer and nonluminescent exciplex formation. To determine the mechanism of PL quenching, an effective method is the lifetime measurement as a function of the quencher concentration. It has been shown that Au_{25} NCs have a core/semiring structure and exhibit a structure correlated PL evolution which

includes prompt fluorescence in a ns timescale and delayed fluorescence in a μs timescale.[16-17, 40, 45] A shorter lifetime component was observed and the amplitude of the μs component decreases with an increasing GO concentration, as shown in Figure 2. Therefore the possibility of static quenching can be ruled out. In addition, there is no any new feature is found in the absorption spectrum of the GO-Au_{25} mixture, compared with Au_{25} NCs and GO. This further supports that the PL quenching is dynamic. The exclusion of exciplex formation was discussed later in a TA measurement.

Basically, energy transfer is one of the possible mechanisms for the Au_{25} NCs PL quenching. Chen et al. showed a d^{-4} rate of energy transfer in CdSe/ZnS nanocrystal in contact with graphene sheet.[46] For 400 nm excitation both Au_{25} NCs and GO can be excited according to their absorption spectra. It should be noted that the PL of GO in the green and blue region was evidently quenched with adding Au_{25} NCs, as shown in figure 1b and the inset. Therefore, the energy transfer can be ruled out because of PL quenching in both donor and acceptor simultaneously. If Au_{25} NCs accept the energy its PL will not quench, and if GO is an acceptor then the population of the excited electron must increase then PL is enhanced. Further evidences from ultrafast transient absorption and upconversion PL could further validate this observation. The possible mechanisms include an additional deactivation of the excited electrons in lowest unoccupied molecular orbital (LUMO) of Au_{25} NCs via electron transfer; or additional electrons injecting to the HOMO of the excited Au_{25} NCs. At a higher GO concentration, a very fast decay appears that is beyond the resolution of the TCSPC system (<300 ps), which indicates that the electron transfer between Au_{25} NCs and GO has a very high rate; similar to that in metal- quantum dots (QDs) systems in subpicoseconds to picoseconds.[23-24, 26, 47]

Figure 3 shows PL evolution of Au_{25} NCs-GO nanocomposites measured by the ultrafast upconversion technique. With increasing GO concentration the PL evolution becomes significantly faster. The evolution can be well fitted by a bi-exponential function

$I(t) = A_1 \exp(-t/\tau_1) + A_2 \exp(-t/\tau_2)$. The fitting parameters were extracted and tabulated in Table 1. For pure Au_{25} NCs the evolution includes fast and slow components with lifetimes of 0.8 and 23 ps, respectively; and an average lifetime $\langle\tau\rangle = (A_1\tau_1 + A_2\tau_2)/(A_1 + A_2)$ of 11 ps. When GO was added the lifetimes significantly decrease. The apparent rate constants of electron transfer could be estimated using [37, 47]

$$k_{ET} = 1/\tau_{(Au\,NCs-GO)} - 1/\tau_{(Au\,NCs)} \quad (1)$$

where $\tau_{(Au\,NCs-GO)}$ and $\tau_{(Au\,NCs)}$ are the lifetimes in Au_{25} NCs-GO and Au_{25} NCs, respectively. The electron transfer rate was determined to be 0.49×10^{12} s^{-1} at a concentration of 2 mg/ml.

As aforementioned, the PL components from both Au_{25} NCs and GO are quenched simultaneously with formation of Au_{25}-GO nanocomposites. And Au_{25} NCs and GO can absorb incident photons of 400 nm. Hence, it is necessary to consider two directional electron transfers, the GO acts as either a donor or an acceptor. To acquire the further insight into the detailed mechanism, we performed ultrafast transient absorption (TA) for Au_{25} NCs, GO and the Au_{25}-GO, as shown in Figure 4 for the TA spectra. Immediately after a laser pulse, GO exhibits broad excited state absorption (ESA) in the visible region,[41, 48] whereas Au_{25} NCs show very low ESA in a ps time scale. Recently, Wang *et al*. demonstrated that the broad ESA is resulted from the directly excited sp^3 matrix states (oxygen-containing functional groups) in GO using TA spectroscopy.[48] In Au_{25} NCs–GO the TA basically exhibit similar feature with that in GO with decreased amplitude. The TA spectra clearly indicate that the excited electron population of GO decreases significantly due to Au_{25} NCs, which suggests the excited electrons transfer from the excited state of GO to Au_{25} NCs. The only possible pathway of electron transfer is that the HOMO of the excited Au_{25} NCs accepts the electrons from the excited states of GO. As shown in Scheme 1, GO is the donor and Au_{25} NC is the acceptor in this

process. To further confirm this claim, we measured the TA spectra with increased excitation intensity.

Furthermore, photon induced non-luminescent exciplex formation is a possibility mechanism for the dynamic PL quenching, in which Au_{25} and/or GO are excited and form a non-luminescent exciplex. In this case, the exciplex should have a different electron structure from those of GO and Au NCs; and thus some features can likely observe during its formation and separation in TA experiment. Obviously, the TA experiments do not support this.

Moreover, we compare the TA time traces of GO and GO-Au_{25} NCs, as shown in Figure 5. Evidently, using single exponential function fitting we acquired their decay time, 2.20 and 4.88 ps for GO-Au_{25} NCs and GO, respectively. The variation is attributed to the additional pathway to Au_{25} NCs, with transfer rate of $0.25\times10^{12}\ s^{-1}$, estimated by equation 1. It should be noted that this transfer rate is smaller than that acquired from the PL upconversion measurement. Taking into account the fact that the ESA population of GO decreases in a broad visible region. This indicates the electrons transfer into Au_{25} NCs is not selective; instead, from various excited states. Luo et al. showed that GO contains a wide range of local band gap minima,[49] Shang *el al.* proposed many localized states in the conduction and valence bands,[41] consistent with the observed broad emission and absorption spectra. In Au_{25} NCs all of the accepted electrons will reflect in the population of the HOMO. In other words, the observed variation of electron population in Au_{25} NCs is arisen from the sum of all accepted electrons from GO's excited states. Therefore, it is reasonable that the electron transfer rate in Au_{25} NCs is larger than that extracted from the TA in any single wavelength.

Au_{10} NCs-GO nanocomposites

Figure 6a shows the PL spectra of the Au_{10} NCs-GO mixture as a function of the GO concentration. The PL intensity monotonically decreases upon increasing the concentration, suggesting the strong

interaction between Au_{10} NCs and GO. The S-V plot approximately exhibits a linearity and the quenching constant was determined to be 2.02×10^3 $(\mu g/mL)^{-1}$, larger than that in Au_{25} NCs-GO. To determine whether the PL quenching is either electron or energy transfer in nature, we review the detailed PL quenching. As shown in Figure 6a, the PL from GO in the red was quenched upon mixing with Au_{10}/His; in addition to the PL quenching of Au_{10} NCs in the blue. Therefore, energy transfer can be ruled out from the possible PL quenching mechanism.

It is evident that a shorter lifetime component was observed in Au_{10} NCs-GO with increasing GO concentrations, as shown in Figure 7. A very fast decay evidently appears in PL evolutions at a higher GO concentration, which indicates that the electron transfer in Au_{10} NCs-GO nanocomposite has a very high rate. Figure 8 shows PL evolutions of Au_{10} NCs-GO nanocomposites with various concentrations in the fs-ps range. The PL evolution becomes significantly faster with an increasing GO concentration. We obtained the decay constants by fitting PL evolutions, as tabulated in Table 2. For pure Au_{10} NCs the evolution include fast and slow components with time constants of 1.77 and 16.8 ps, respectively. When GO was added an ultrafast component appears in addition to the other slower components. The lifetime of the fastest component is approximately independent on the concentration but the relative amplitude is dependent on the concentration. At a concentration of 0.5 mg/ml the slowest component becomes too weak to be detected. The fastest component can be attributed to the additional relaxation pathway, that is, electron transfer between the excited Au_{10} NCs and GO. The time constant was determined as 240 fs, corresponding to an electron transfer rate of 4.17×10^{12} s^{-1}. It should be noted that this rate is significantly larger than that in Au_{25} NCs-GO nanocomposite, suggesting stronger interactions in this nanocomposite. Moreover, we compared the TA spectra in Au_{10} NCs, GO and Au_{10} NCs-GO nanocomposites. As shown in Figure 9, the ESA of GO decreases significantly in the visible region upon formation of Au_{10} NCs–GO nanocomposites. This indicates the electron transfers from the excited states of GO to the HOMO of Au_{10} NCs.

The electron structures of Au NCs and GO, as well as the correlation with fluorescence, have been investigated theoretically and experimentally, although the details are still unclear.[10, 16-17, 31, 41, 45, 50-53] It was suggested the transition between LUMO+1/LUM+2 and HOMO is responsible for the fluorescence in Au_{25}.[17, 45] Kogo et al. determined the potential value of HOMOs and LUMOs by photoelectrochemical analysis.[31] Shang et al. suggested localized excited states in conduction and valance bands are responsible for the observed fluorescence in GO.[41] Based on these studies, the energy diagram is shown in Figure 10.

It should be emphasized that the rate of electron transfer in Au_{10} NCs-GO, $4.17\times10^{12}\ s^{-1}$, is greater than that in Au_{25}-GO, $0.49\times10^{12}\ s^{-1}$. According to the Marcus theory, electron transfer from GO to Au NCs, the total electron transfer rate K_{ET} can be expressed as[47, 54]

$$K_{ET}=\frac{2\pi}{\hbar}\int_{-\infty}^{\infty}dE\,\rho(E)\,|\bar{H}(E)|^2\,\frac{1}{\sqrt{4\pi\lambda k_B T}}\exp[-\frac{(\lambda+\Delta G_0+E)^2}{4\lambda k_B T}] \qquad (2)$$

where $\Delta G_0=E_{GO}-E_{Au}$ is free energy driving force; $\bar{H}(E)$ and $\rho(E)$ are the average electronic coupling and the density of states at energy E; λ is the total reorganization energy; k_B and T are Boltzmann's constant and absolute temperature. Free energy driving force, the energy difference between donor and acceptor, dominates electron transfer rate. The distance between donor and acceptor will also significantly influence the transfer rate. Compared to Au_{25} NCs, Au_{10} NCs have fewer Au atoms in each cluster. According to the jellium model, Au_{10} NCs will exhibit a larger band gap owing to the stronger quantum confinement. As shown in Figure 10, the energy difference between the excited states of GO and the HOMO of Au_{10} is evidently larger in GO-Au_{10} than that in GO-Au_{25}. In addition, BSA has a significantly larger size than that of histidine, which suggests Au_{10}/His can contact GO more tightly than Au_{25}/BSA. The large driving force together with a smaller distance between the donor and acceptor in turn results in a larger electron transfer rate.

To obtain the further insight into the interaction between Au NCs and GO, it is necessary to compare the interaction between Au NCs and some usually used electron acceptors, such as multiwall carbon nanotube (MWCNT) and TiO_2 nanoparticles. Upon adding MWCNT, the PL of Au_{10} and Au_{25} NCs was quenched and the S-V plot exhibits exponential upward (Figure S2). Therefore, either dynamic and/or static quenching are the possible mechanisms for the PL quenching. To confirm the quenching mechanism we measured the PL lifetime using TCSPC technique. As shown in Figure S3, the PL evolutions of Au_{10} NCs-MWCNT and Au_{25} NCs-MWCNT do not exhibit discernible variation with changing MWCNT concentrations. Therefore, the PL quenching is ascribed to a static quenching, that is, ground state quenching. The apparent static component is due to the quencher being adjacent to the fluorophore at the moment of excitation, so called sphere of action. These spatially closed fluorophore-quencher pairs are immediately quenched, and are referred to as dark complexes. It should be emphasized that such a static quenching does not form a stable Au NCs-MWCNT complex.[44] There is no new absorption band formation and the absorption spectrum of the mixture is simply the linear overlying of the individual absorption of Au NCs and MWCNT, as shown in Figure S4. The similar static quenching was observed in P3HT and MWCNT,[55] as well as rhodamine B and CNTs pairs.[56] In the case of Au NCs and TiO_2 nanoparticles (NP), as shown in Figure S5, the PL was not evidently quenched for both Au_{10} and Au_{25} NCs when mixing with TiO_2 NP. The lifetime measurement confirmed that there is no obvious variation in the mixture of Au NCs and TiO_2 NPs, (Figure S6). This indicates a weak interaction occurs between Au NCs and TiO_2 NPs. Therefore, to construct an Au NCs - TiO_2 nanocomposite it is necessary to functionalize Au NCs and/or TiO_2 NPs. Recently, Kamat *et al.* also demonstrated that surface chemistry plays a major role in controlling K_{ET} at the interface of composite, as well as interparticle separation.[57] The TEM images confirm both Au_{25} and Au_{10} can tightly attach onto GO, which results in a strong interaction between Au NCs and GO. It has been shown that GO has strong hydrophobic interaction and unique surface irreversible protein adsorption ability.[4-5] On the other hand, an electrostatic force can drive Au NCs

spontaneously immobilization on GO when Au NCs mix with GO.[58] In this process Au NCs can effectively self-assemble to anchor into GO and form a stable nanocomposite due to the electrostatic interaction. However, it is still hard to identify either electrostatic or hydrophobic interaction is dominant. Further investigation nevertheless is required to clarify the detailed interaction in the nanocompositions. In Au NCs-GO nanocomposite electron can effectively transfer from GO to the excited Au NCs due to the enhanced interaction.[47]

Conclusion

In summary, electron transfer dynamics has been investigated using steady state and time-resolved spectroscopy. The PL of Au NCs is evidently quenched when GO-Au NCs nanocomposites form. An unusual electron transfer was confirmed from the excited states of GO to the HOMO of the excited AuNCs, for both Au_{10}/His-GO and Au_{25}/BSA-GO. The rates of electron transfer were determined using ultrafast upconversion PL as 0.49×10^{12} s^{-1} and 4.17×10^{12} s^{-1} in Au_{25}-GO and Au_{10}-GO nanocomposites, respectively. This ultrafast electron transfer in Au_{10}-GO nanocomposites was ascribed to the larger driving force (energy difference) and smaller size of ligand (histidine), compared with in Au_{25}-GO. This finding suggests that such Au NC-GO nanocomposites can be very useful to construct functionalized nanocomposites based on excellent electron donor of GO for the enhanced visible light absorption photovoltaic and catalysis applications.

Experimental Section

Synthesis of Au NCs and materials

The Au NCs used in this study were synthesised using the biomineralized approach, as described previously.[10-11, 18, 39] Typically, 5 mL of 10 mM $HAuCl_4$ was mixed with 5 mL of 50mg/mL bovine serum albumin (BSA, 66.7 kDa) and kept at 37℃ overnight in an incubator while the pH was at 11 for Au_{25} (ca. 200 μM). For Au_{10}@histidine synthesis, 1mL of 10 mM $HAuCl_4$ was mixed with 3 mL of 0.1 M histidine and kept at 25℃ for two hours in the incubator (ca. 250 μM). Single layer

graphene oxide (purity >80%, flake size 0.5-5 μm) were obtained from Nanocs. -COOH modified MWCNT (diameter ~1.5 nm, length 1-5 um) was purchased from Golden Innovation Business. TiO_2 NPs (diameter ~20nm, anatase) was purchased from CBT. In the PL and TRPL experiments the absorption of the mixtures has been corrected by adding exactly the same volume of solutions with different concentrations or DI water. All the mixtures were allowed to stand for 60 min for further optical measurements to have a stable PL intensity, as shown in Figure S7.

Spectroscopic measurements

Absorption and fluorescence spectra were recorded using the JASCO UV/Visible (V-670) and fluorescent (FP-6300) spectrophotometer, respectively. The PL lifetimes were measured by TCSPC technique on Microtime-200 (Picoquant). The femtosecond (fs) time-resolved PL experiments were performed on an up-conversion fluorimeter (Fluomax, IB Photonics), the details was described in the previously publication.[59] The excitation source is a 400 nm pulsed laser with 100 fs duration and an 80 MHz repetition rate. The fs pump-probe experiments were performed with a transient absorption spectrometer (FemtoFrame II, IB Photonics). The excitation source is a 400 nm pulse by an OPA laser (TOPAS, Spectra Physics) with 100 fs duration and 1 kHz repetition rate. The probe beam of white light continuum was generated by focusing the 1 kHz Ti:Sapphire amplified laser (Spitfire, Spectra Physics) into BBO crystal, and detected by a polychromator-CCD. All of the measurements were performed at room temperature.

Acknowledgement

This Program has been supported by the Australian Government through the Australian Renewable Energy Agency (ARENA). The authors acknowledge the financial support by Academia Sinica and National Science Council (NSC) of Taiwan under the programs NSC99-2221-E-001-002-MY3, NSC99-2113-M-001-023-MY3, and NSC101-2113-M-030-008.

Notes and References

Electronic Supplementary information (ESI) available: PL and lifetime comparison in Au NCs-MWCNT and Au NCs-TiO_2 NPs.

(1) Bolotin, K. I.; Sikes, K.; Jiang, Z.; Klima, M.; Fudenberg, G.; Hone, J.; Kim, P.; Stormer, H. Ultrahigh electron mobility in suspended graphene. *Solid State Communications.* 2008, *146*, 351-355.

(2) Wassei, J. K.; Kaner, R. B. Graphene, a promising transparent conductor. *Materials today.* 2010, *13*, 52-59.

(3) Zhao, X.; Liu, Z. B.; Yan, W. B.; Wu, Y. P.; Zhang, X. L.; Chen, Y. S.; Tian, J. G. Ultrafast carrier dynamics and saturable absorption of solution-processable few-layered graphene oxide. *Appl. Phys. Lett.* 2011, *98*, 121905.

(4) Zuo, X.; He, S.; Li, D.; Peng, C.; Huang, Q.; Song, S.; Fan, C. Graphene oxide-facilitated electron transfer of metalloproteins at electrode surfaces. *Langmuir.* 2009, *26*, 1936-1939.

(5) Song, Y.; Qu, K.; Zhao, C.; Ren, J.; Qu, X. Graphene oxide: intrinsic peroxidase catalytic activity and its application to glucose detection. *Adv. Mater.* 2010, *22*, 2206-2210.

(6) Yu, P.; Wen, X. M.; Toh, Y.-R.; Lee, Y.-C.; Huang, K.-Y.; Huang, S.; Shrestha, S.; Conibeer, G.; Tang, J. Efficient Electron Transfer in Carbon Nanodot-Graphene Oxide Nanocomposites. *Scientific Reports.* 2013, In press.

(7) Loh, K. P.; Bao, Q.; Eda, G.; Chhowalla, M. Graphene oxide as a chemically tunable platform for optical applications. *Nature chemistry.* 2010, *2*, 1015-1024.

(8) Eda, G.; Chhowalla, M. Chemically Derived Graphene Oxide: Towards Large-Area Thin-Film Electronics and Optoelectronics. *Adv. Mater.* 2010, *22*, 2392-2415.

(9) Zheng, J.; Nicovich, P. R.; Dickson, R. M. Highly Fluorescent Noble Metal Quantum Dots. *Ann. Rev. Phys. Chem.* 2007, *58*, 409-431.

(10) Yu, P.; Wen, X.; Toh, Y. R.; Tang, J. Temperature Dependent Fluorescence in Au10 Nanoclusters. *J. Phys. Chem. C.* 2012, *116*, 6567-6571.

(11) Wen, X.; Yu, P.; Toh, Y.-R.; Tang, J. Quantum Confined Stark Effect in Au8 and Au25 Nanoclusters. *J. Phys. Chem. C.* 2013, *117*, 3621-3626.

(12) Wu, Z.; Jin, R. On the Ligand's Role in the Fluorescence of Gold Nanoclusters. *Nano Lett.* 2010, *10*, 2568-2573.

(13) Zheng, J.; Zhang, C. W.; Dickson, R. M. Highly fluorescent, water-soluble, size-tunable gold quantum dots. *Phys. Rev. Lett.* 2004, *93*, 077402

(14) Parker, J. F.; Fields-Zinna, C. A.; Murray, R. W. The Story of a Monodisperse Gold Nanoparticle: Au(25)L(18). *Acc. Chem. Res.* 2010, *43*, 1289-1296.

(15) Aikens, C. M. Origin of Discrete Optical Absorption Spectra of M25 (SH) 18- Nanoparticles

(M= Au, Ag). *J. Phys. Chem. C.* 2008, *112*, 19797-19800.
(16) Zhu, M.; Aikens, C. M.; Hollander, F. J.; Schatz, G. C.; Jin, R. Correlating the crystal structure of a thiol-protected Au25 cluster and optical properties. *J. Am. Chem. Soc.* 2008, *130*, 5883-5885.
(17) Wen, X.; Yu, P.; Toh, Y.-R.; Tang, J. Structure-Correlated Dual Fluorescent Bands in BSA-Protected Au25 Nanoclusters. *J. Phys. Chem. C.* 2012, *116*, 11830-11836.
(18) Xie, J.; Zheng, Y.; Ying, J. Y. Protein-directed synthesis of highly fluorescent gold nanoclusters. *J. Am. Chem. Soc.* 2009, *131*, 888-889.
(19) Maity, P.; Xie, S.; Yamauchi, M.; Tsukuda, T. Stabilized gold clusters: from isolation toward controlled synthesis. *Nanoscale.* 2012, *4*, 4027-4037.
(20) Yuan, X.; Luo, Z.; Zhang, Q.; Zhang, X.; Zheng, Y.; Lee, J. Y.; Xie, J. Synthesis of highly fluorescent metal (Ag, Au, Pt, and Cu) nanoclusters by electrostatically induced reversible phase transfer. *ACS nano.* 2011, *5*, 8800-8808.
(21) Wu, Z.; Gayathri, C.; Gil, R. R.; Jin, R. Probing the Structure and Charge State of Glutathione-Capped Au25 (SG) 18 Clusters by NMR and Mass Spectrometry. *J. Am. Chem. Soc.* 2009, *131*, 6535-6542.
(22) Akola, J.; Walter, M.; Whetten, R. L.; Hakkinen, H.; Gronbeck, H. On the structure of thiolate-protected Au25. *J. Am. Chem. Soc.* 2008, *130*, 3756-3757.
(23) Devadas, M. S.; Kwak, K.; Park, J.-W.; Choi, J.-H.; Jun, C.-H.; Sinn, E.; Ramakrishna, G.; Lee, D. Directional Electron Transfer in Chromophore-Labeled Quantum-Sized Au(25) Clusters: Au(25) as an Electron Donor. *J. Phys. Chem. Lett.* 2010, *1*, 1497-1503.
(24) Liu, Z.; Zhu, M.; Meng, X.; Xu, G.; Jin, R. Electron Transfer between [Au25 (SC2H4Ph) 18]− TOA+ and Oxoammonium Cations. *J. Phys. Chem. Lett.* 2011, *2*, 2104-2109.
(25) Chen, Y.-S.; Choi, H.; Kamat, P. V. Metal Cluster Sensitized Solar Cells. A New Class of Thiolated Gold Sensitizers Delivering Efficiency Greater Than 2%. *J. Am. Chem. Soc.* 2013, *135*, 8822-8825.
(26) Chen, W. T.; Hsu, Y. J.; Kamat, P. V. Realizing Visible Photoactivity of Metal Nanoparticles. Excited State Behavior and Electron Transfer Properties of Silver (Ag8) Clusters. *J. Phys. Chem. Lett.* 2012, *3*, 2493-2499.
(27) Liu, Z.; Xu, Q.; Jin, S.; Wang, S.; Xu, G.; Zhu, M. Electron transfer reaction between Au25 nanocluster and phenothiazine-tetrachloro-p-benzoquinone complex. *Int. J. Hydrogen Energy.* 2013, *38*, 16722–16726.
(28) Antonello, S.; Hesari, M.; Polo, F.; Maran, F. Electron transfer catalysis with monolayer protected Au25 clusters. *Nanoscale.* 2012, *4*, 5333-5342.
(29) Yu, C.; Li, G.; Kumar, S.; Kawasaki, H.; Jin, R. Stable Au25 (SR) 18/TiO2 Composite Nanostructure with Enhanced Visible Light Photocatalytic Activity. *J. Phys. Chem. Lett.* 2013, *4*, 2847-2852.
(30) Sakai, N.; Tatsuma, T. Photovoltaic Properties of Glutathione-Protected Gold Clusters Adsorbed on TiO2 Electrodes. *Adv. Mater.* 2010, *22*, 3185-3188.

(31) Kogo, A.; Sakai, N.; Tatsuma, T. Photoelectrochemical analysis of size-dependent electronic structures of gold clusters supported on TiO2. *Nanoscale.* 2012, *4*, 4217-4221.
(32) Liu, C. J.; Zhang, P.; Tian, F.; Li, W. C.; Li, F.; Liu, W. G. One-step synthesis of surface passivated carbon nanodots by microwave assisted pyrolysis for enhanced multicolor photoluminescence and bioimaging. *J. Mater. Chem.* 2011, *21*, 13163-13167.
(33) Chen, W.; Chen, S.; Qi, D. C.; Gao, X. Y.; Wee, A. T. S. Surface transfer p-type doping of epitaxial graphene. *J. Am. Chem. Soc.* 2007, *129*, 10418-10422.
(34) Voggu, R.; Das, B.; Rout, C. S.; Rao, C. Effects of charge transfer interaction of graphene with electron donor and acceptor molecules examined using Raman spectroscopy and cognate techniques. *J. Phys.: Condens. Matter.* 2008, *20*, 472204.
(35) Kozhemyakina, N. V.; Englert, J. M.; Yang, G.; Spiecker, E.; Schmidt, C. D.; Hauke, F.; Hirsch, A. Non-Covalent Chemistry of Graphene: Electronic Communication with Dendronized Perylene Bisimides. *Adv. Mater.* 2010, *22*, 5483-5487.
(36) Costa, R. D.; Malig, J.; Brenner, W.; Jux, N.; Guldi, D. M. Electron Accepting Porphycenes on Graphene. *Adv. Mater.* 2013, *25*, 2600–2605.
(37) Bang, J. H.; Kamat, P. V. CdSe quantum dot–fullerene hybrid nanocomposite for solar energy conversion: electron transfer and photoelectrochemistry. *ACS nano.* 2011, *5*, 9421-9427.
(38) Hyun, B.-R.; Zhong, Y.-W.; Bartnik, A. C.; Sun, L.; Abruña, H. D.; Wise, F. W.; Goodreau, J. D.; Matthews, J. R.; Leslie, T. M.; Borrelli, N. F. Electron injection from colloidal PbS quantum dots into titanium dioxide nanoparticles. *Acs Nano.* 2008, *2*, 2206-2212.
(39) Yang, X.; Shi, M.; Zhou, R.; Chen, X.; Chen, H. Blending of HAuCl4 and histidine in aqueous solution: a simple approach to the Au10 cluster. *Nanoscale.* 2011, *3*, 2596-2601.
(40) Yu, P.; Wen, X.; Toh, Y.-R.; Huang, J.; Tang, J. Metallophilic Bond-Induced Quenching of Delayed Fluorescence in Au25@BSA Nanoclusters. *Particle & Particle Systems Characterization.* 2013, *30*, 467-472.
(41) Shang, J.; Ma, L.; Li, J.; Ai, W.; Yu, T.; Gurzadyan, G. G. The Origin of Fluorescence from Graphene Oxide. *Scientific Reports.* 2012, *2*, 792.
(42) Liu, F.; Jang, M. H.; Ha, H. D.; Kim, J. H.; Cho, Y. H.; Seo, T. S. Facile Synthetic Method for Pristine Graphene Quantum Dots and Graphene Oxide Quantum Dots: Origin of Blue and Green Luminescence. *Adv. Mater.* 2013, *25*, 3657-3662.
(43) Dong, H.; Gao, W.; Yan, F.; Ji, H.; Ju, H. Fluorescence resonance energy transfer between quantum dots and graphene oxide for sensing biomolecules. *Analytical chemistry.* 2010, *82*, 5511-5517.
(44) Yu, P.; Wen, X.; Toh, Y.-R.; Lee, Y.-C.; Tang, J. Optical properties of gold particle-cluster core–satellite nanoassemblies. *RSC Advances.* 2013, *3*, 19609-19616.
(45) Wen, X.; Yu, P.; Toh, Y.-R.; Hsu, A.-C.; Lee, Y.-C.; Tang, J. Fluorescence Dynamics in BSA Protected Au25 Nanoclusters. *J. Phys. Chem. C.* 2012, *116*, 19032-19038.
(46) Chen, Z.; Berciaud, S.; Nuckolls, C.; Heinz, T. F.; Brus, L. E. Energy transfer from individual

semiconductor nanocrystals to graphene. *ACS nano.* 2010, *4*, 2964-2968.
(47) Tvrdy, K.; Frantsuzov, P. A.; Kamat, P. V. Photoinduced electron transfer from semiconductor quantum dots to metal oxide nanoparticles. *PNAS.* 2011, *108*, 29-34.
(48) Wang, L.; Wang, H. Y.; Wang, Y.; Zhu, S. J.; Zhang, Y. L.; Zhang, J. H.; Chen, Q. D.; Han, W.; Xu, H. L.; Yang, B. Direct Observation of Quantum□Confined Graphene-Like States and Novel Hybrid States in Graphene Oxide by Transient Spectroscopy. *Adv. Mater.* 2013, 10.1002/adma.201302927.
(49) Luo, Z.; Vora, P. M.; Mele, E. J.; Johnson, A.; Kikkawa, J. M. Photoluminescence and band gap modulation in graphene oxide. *Appl. Phys. Lett.* 2009, *94*, 111909-111909-3.
(50) Aikens, C. M. Geometric and Electronic Structure of Au25 (SPhX) 18−(X= H, F, Cl, Br, CH3, and OCH3). *J. Phys. Chem. Lett.* 2010, *1*, 2594-2599.
(51) Wen, X.; Yu, P.; Toh, Y.-R.; Ma, X.; Huang, S.; Tang, J. Fluorescence origin and spectral broadening mechanism in atomically precise Au 8 nanoclusters. *Nanoscale.* 2013, *5*, 10251-10257.
(52) Lecoultre, S.; Rydlo, A.; Félix, C.; Buttet, J.; Gilb, S.; Harbich, W. UV–visible absorption of small gold clusters in neon: Aun (n= 1–5 and 7–9). *J. Chem. Phys.* 2011, *134*, 074302-8.
(53) Koppen, J. V.; Hapka, M.; Szczęśniak, M. M.; Chałasiński, G. Optical absorption spectra of gold clusters Aun (n= 4, 6, 8, 12, 20) from long-range corrected functionals with optimal tuning. *J. Chem. Phys.* 2012, *137*, 114302-15.
(54) Anderson, N. A.; Lian, T. Ultrafast electron transfer at the molecule-semiconductor nanoparticle interface. *Annu. Rev. Phys. Chem.* 2005, *56*, 491-519.
(55) Goutam, P. J.; Singh, D. K.; Iyer, P. K. Photoluminescence Quenching of Poly (3-hexylthiophene) by Carbon Nanotubes. *The Journal of Physical Chemistry C.* 2012, *116*, 8196-8201.
(56) Ahmad, A.; Kurkina, T.; Kern, K.; Balasubramanian, K. Applications of the static quenching of rhodamine B by carbon nanotubes. *ChemPhysChem.* 2009, *10*, 2251-2255.
(57) Hines, D. A.; Kamat, P. V. Quantum Dot Surface Chemistry: Ligand Effects and Electron Transfer Reactions. *J. Phys. Chem. C.* 2013, *117*, 14418–14426.
(58) Tao, Y.; Lin, Y.; Huang, Z.; Ren, J.; Qu, X. Incorporating Graphene Oxide and Gold Nanoclusters: A Synergistic Catalyst with Surprisingly High Peroxidase-Like Activity Over a Broad pH Range and its Application for Cancer Cell Detection. *Adv. Mater.* 2013, *25*, 2594–2599.
(59) Wen, X.; Yu, P.; Toh, Y. R.; Hao, X.; Tang, J. Intrinsic and Extrinsic Fluorescence in Carbon Nanodots: Ultrafast Time-Resolved Fluorescence and Carrier Dynamics. *Advanced Optical Materials.* 2013, *1*, 173-178.

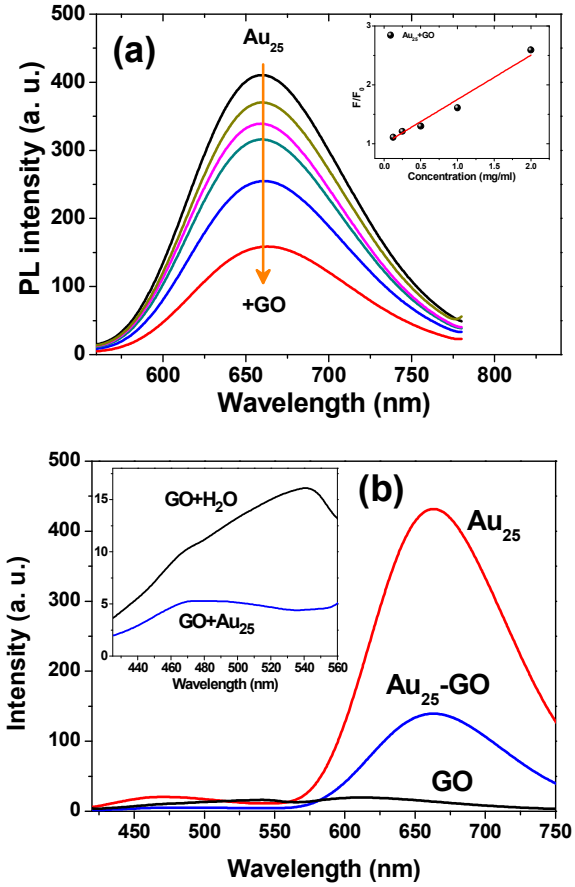

Figure 1. (a) The PL spectra of Au_{25} NCs as a function of the GO concentration; inset: the corresponding Stern-Volmer plot. (b) the PL spectra of Au_{25} NCs, GO and Au_{25}-GO nanocomposites; inset shows the PL spectra of GO and GO-Au_{25} NCs in the green/blue region with a corrected absorption. Excitation at 400 nm.

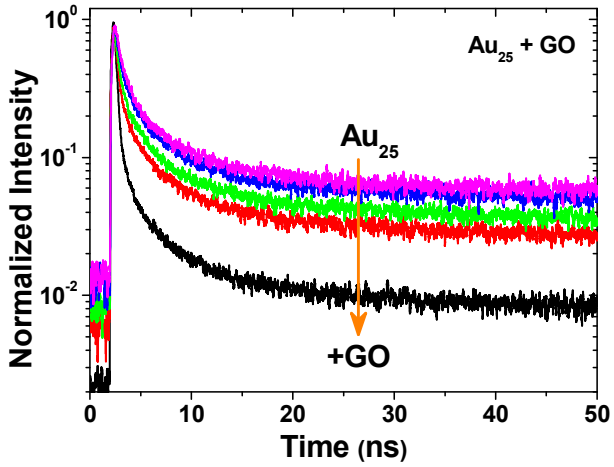

Figure 2. The PL evolutions of GO-Au_{25} NCs as a function of GO concentration at 650 nm, in ns timescale with 400 nm excitation.

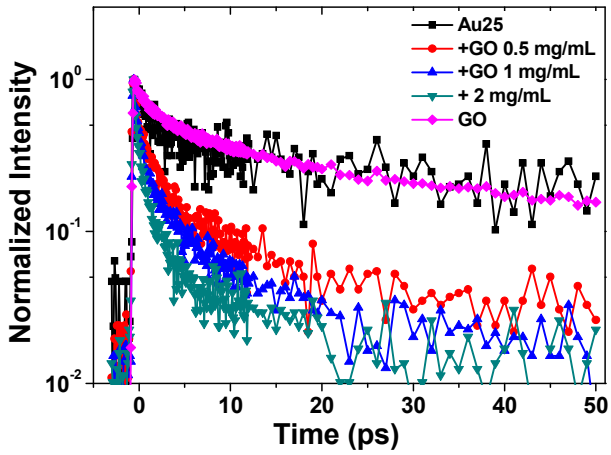

Figure 3. The PL evolutions of GO-Au_{25} NCs with various GO concentrations at 650 nm in ps timescale.

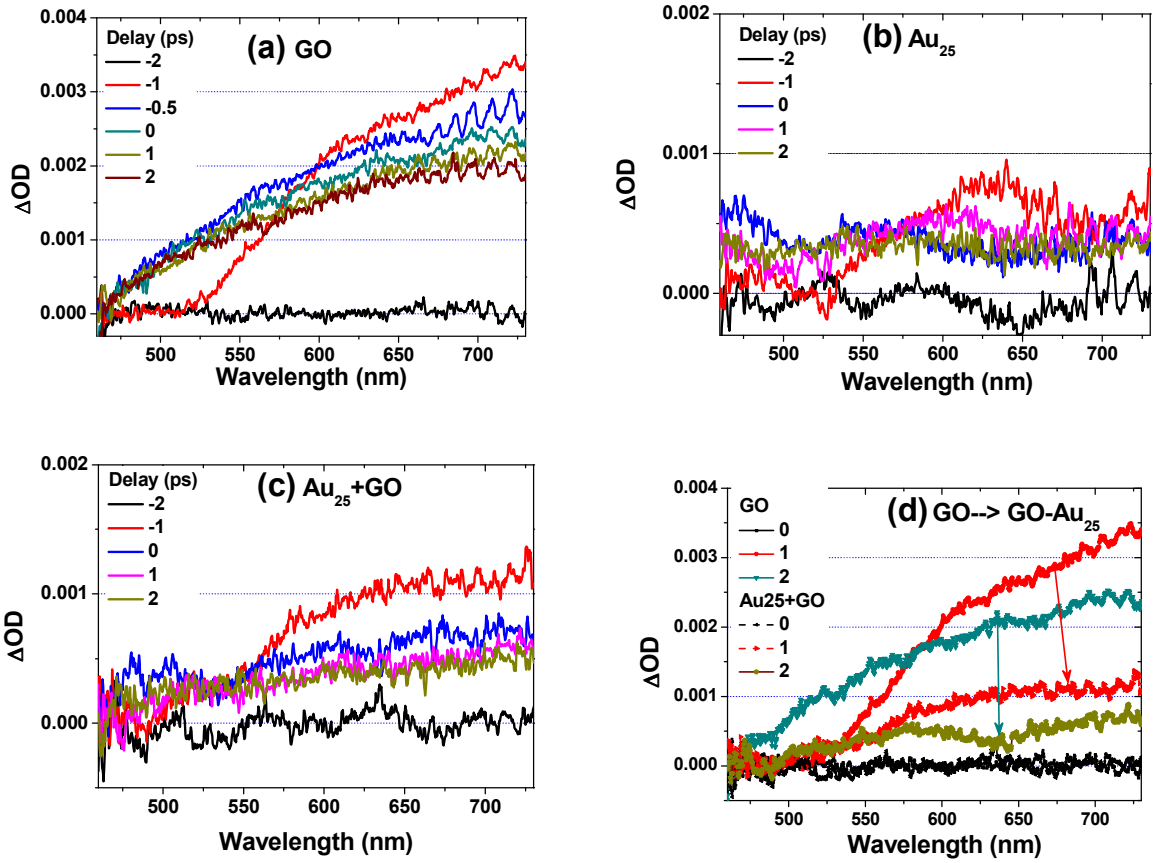

Figure 4. Transient absorption spectra of (a) GO, (b) Au_{25} NCs, (c) Au_{25}-GO, and (d) comparison between GO and Au_{25}-GO.

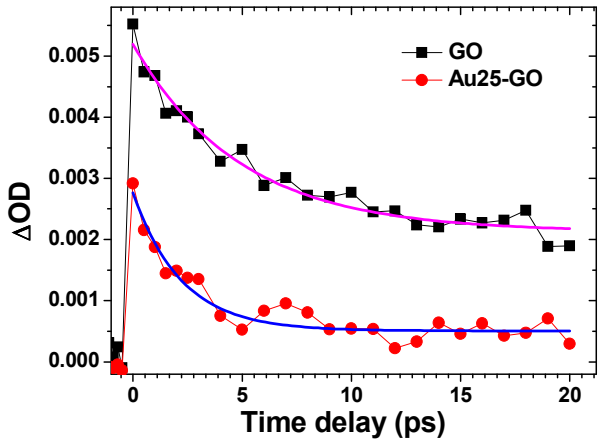

Figure 5. Decay traces of transient absorption for GO and Au_{25}-GO at 650 nm.

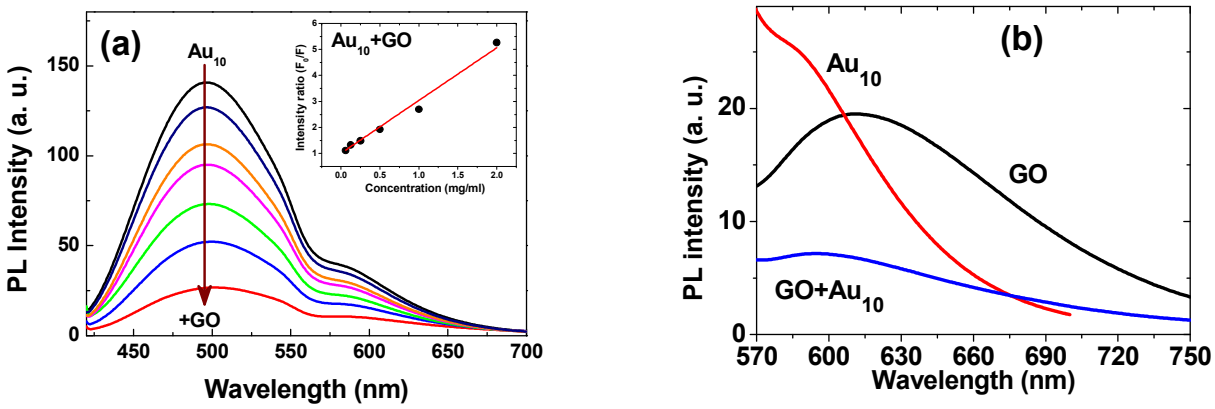

Figure 6. (a) The PL spectra of Au_{10} NCs as a function of the GO concentrations, inset: the corresponding Stern-Volmer plot ; (b) the PL spectra of GO, Au_{10} NCs and GO-Au_{10}. Excitation at 400 nm.

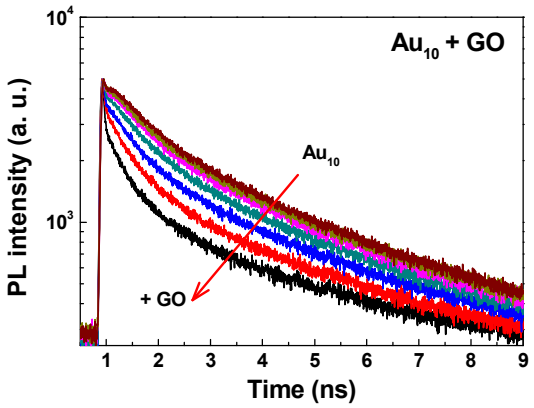

Figure 7. The PL evolutions of GO-Au_{10} NCs at various GO concentrations at 500 nm excited at 400 nm.

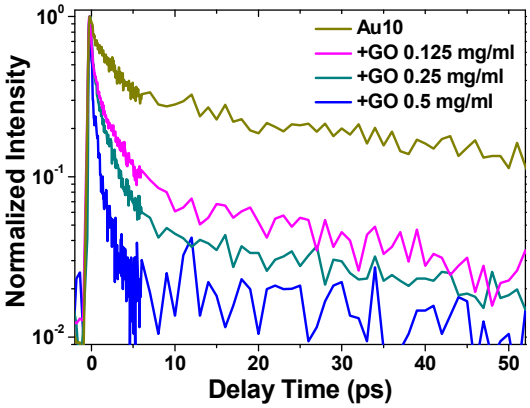

Figure 8. The PL evolutions of GO-Au_{10} NCs as a function of GO concentrations at 500 nm.

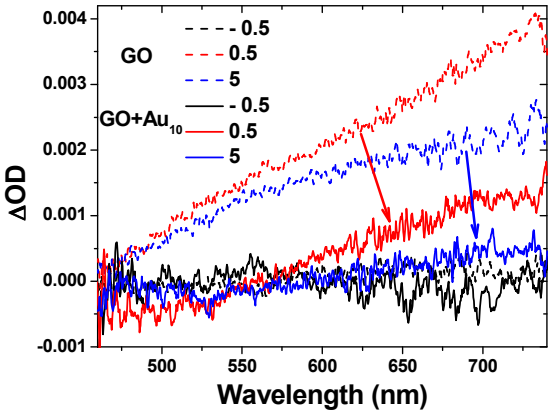

Figure 9. Comparison of transient absorption spectra between GO and Au_{10}-GO nanocomposites.

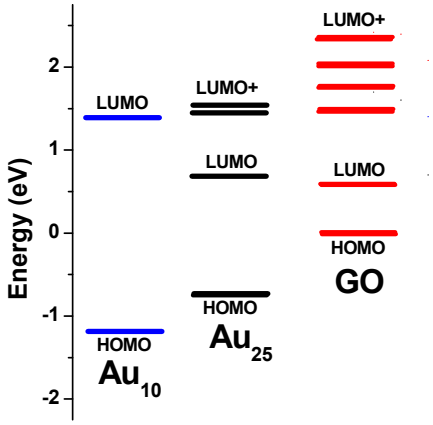

Figure 10. An energy diagram of Au_{10} NCs, Au_{25} NCs and GO.

Table 1. Lifetimes extracted by biexponential fitting from PL evolutions of Au_{25}NCs-GO nanocomposites.

	Au_{25}	+0.5 mg/mL	+1 mg/mL	+2 mg/mL	GO
A1	0.374	0.234	0.220	0.154	0.250
τ_1 (ps)	0.82	0.72	0.60	0.48	1.74
A2	0.311	0.252	0.193	0.160	0.402
τ_2 (ps)	23.4	5.1	5.1	2.9	13.6
$<\tau>$ (ps)	11.08	3.00	2.70	1.72	9.08

Table 2. Lifetimes extracted by exponential fitting in PL evolutions of Au_{10} NCs-GO nanocomposites.

	Au_{10}	+0.125 mg/mL	+0.25 mg/mL	+0.5 mg/mL
A1		0.195	0.424	0.429
τ_1 (ps)		0.31	0.25	0.24
A2	0.357	0.317	0.380	0.220
τ_2 (ps)	1.77	1.97	1.77	1.60
A3	0.288	0.094	0.046	0.004
τ_3 (ps)	16.81	17.02	19.10	14.98

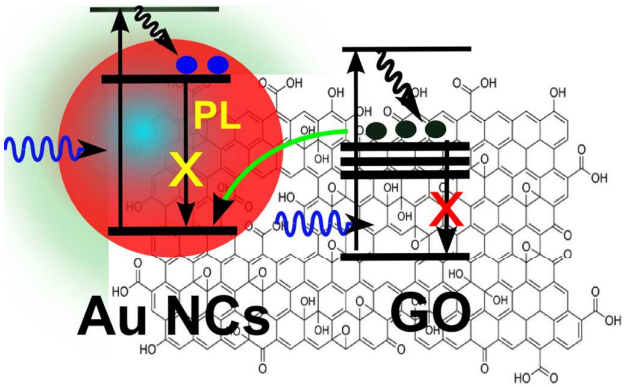

Scheme 1. Electron transfer from the excited states of GO to the HOMO of Au NCs results in PL quenching in both GO-Au_{25} and GO-Au_{10} nanocompositites.

TOC.

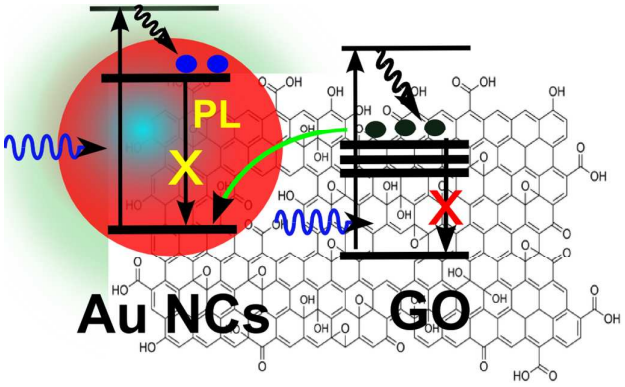

Novel electron transfer results in PL quenching in both graphene oxide-Au_{25} and graphene oxide-Au_{10} nanocompositites.